Quantitation of the Critically Ischemic Zone at Risk During Acute Coronary Occlusion Using PET

Michael Merhige, Dahlia Garza, David Sease, R. Wanda Rowe, Timothy Tewson, Ali Emran, Leonard Bolomey, and K. Lance Gould

Division of Cardiology and the Positron Diagnostic and Research Center, University of Texas Health Science Center at Houston, Texas

Critical myocardial ischemia has been defined experimentally during acute coronary occlusion as flow reduction of 50% or more since cellular ATP depletion begins to occur beyond this flow reduction threshold, placing tissue at risk of cellular injury. To test the hypothesis that critically ischemic fractional left ventricular mass can be measured noninvasively with PET, nine dogs were imaged in a multi-slice positron camera using the perfusion tracer ^{13}N-ammonia, while radiolabeled microspheres were injected into the left atrium during acute coronary occlusion. Images were processed using a 50% threshold and the size of the resulting perfusion defect was expressed as a fraction of total left ventricular image volume. The critically ischemic left ventricular fraction determined in vitro from the microsphere perfusion data, ranged from 5% to 30% of the total left ventricular weight and correlated closely with that determined noninvasively by PET with $r = 0.94$ ($y = 1.05X - 2.0\%$). We conclude that the fraction of left ventricular myocardium rendered critically ischemic during acute coronary occlusion can be measured accurately and noninvasively in vivo using perfusion imaging with positron emission tomography.

J Nucl Med 1991; 32:1581–1586

Positron emission tomography (PET) permits the noninvasive recovery of radiotracer concentration in vivo in an imaged volume of tissue and when used with perfusion tracers such as ^{13}N-ammonia or ^{82}Rb, defines areas of myocardial ischemia (*1–3*). Multi-slice PET cameras, which simultaneously image the entire cardiac volume, allow measurement of the fraction of myocardium rendered ischemic during acute coronary occlusion. From a clinical perspective, this noninvasive quantitative capability could guide decisions regarding aggressive myocardial salvage in patients with both acute and chronic ischemic heart disease.

Received Jul. 31, 1990; revision accepted Mar. 6, 1991.

For reprints contact: Michael E. Merhige, MD, Buffalo Cardiology and Pulmonary Associates, P.C., 5305 Main St., Buffalo, NY 14221.

Flow reductions greater than 50% of normally perfused myocardium result in large decreases in tissue ATP concentration, while milder flow reductions, to levels above 50% of normally perfused tissue, result in little or no decrease in cellular ATP content despite prolonged coronary occlusion in dogs (*4*).

Thus, tissue subjected to flow deprivation greater than 50% has been defined as "critically" ischemic (*4*), since cellular injury in this physiologic zone at risk is both flow and time dependent. Since relative myocardial distribution of ^{13}N-ammonia and ^{82}Rb results from both antegrade and collateral flow (*1–3, 5–9*) in addition to reflecting myocardial oxygen demand through the level of peak uptake in the normally perfused tissue during acute coronary occlusion, PET perfusion imaging is ideally suited for identification of critically ischemic myocardium during coronary occlusion in vivo.

The purpose of this study was to test the hypothesis that the fraction of left ventricular (LV) myocardium rendered critically ischemic during acute coronary occlusion (i.e., subjected to flow reductions of greater than 50% of the peak value in normally perfused tissue) can be accurately measured in vivo with PET.

MATERIALS AND METHODS

Instrumentation

Nine mongrel dogs weighing 25–35 kg underwent anesthetic induction with 20–30 mg/kg of intravenous thiopental prior to acute study. Following endotracheal intubation with a cuffed tube, general anesthesia was maintained with 0.1%–0.5% methoxyflurane (Penthrane), 2 l/min NO_2 and 3 l/min O_2 using a Met-O-Matic veterinary anesthesia machine (Ohio Medical Products). A left thoractomy was performed, the heart was suspended in a pericardial cradle, and a doubled 2-0 silk ligature was placed loosely around the left anterior descending coronary artery (LAD) just after the first or second large diagonal vessel in order to produce larger or smaller ischemic zones. A soft cannula was inserted into the left atrial appendage and secured with a purse-string suture. Short, stiff catheters were placed in the right femoral artery and vein and sutured in place for intravenous drugs and radionuclides, for withdrawal of arterial blood during microsphere (MS) injection, and for monitoring arterial pressure with

an AIL Tech pressure transducer and an Electronics for Medicine recorder.

Radionuclides and Positron Camera

Nitrogen-13-ammonia was produced on a 35-meV Scanditronix positron cyclotron as previously described (*10*). Rubidium-82 was eluted from a ^{82}Sr-generator system (Squibb) (*11*) with normal saline and the dose checked in a CRC-10 dose calibrator (Capintech Inc.). As reported previously (*12*), the University of Texas multi-slice positron camera has 720 cesium fluoride detectors (18 mm diameter by 45 mm long) arranged in 5 rings of 144 detectors each, producing 9 simultaneous image planes encompassing the entire LV volume in the imaging field in a single data acquisition. The inplane reconstruction resolution was 14 mm. FWHM using a medium reconstruction filter and axial resolution was also 14 mm FWHM. The detectors were "wobbled" with a small circular motion of 19.6 mm in diameter in order to improve in-plane sampling. A complete three dimensional multi-slice image of the distribution of radioactivity in the heart was thus obtained in one 10–15-min data acquisition, without moving the animal.

Imaging Protocol

Immediately following surgery, each animal was placed on its right side in the positron camera so that the heart was within the central third of the imaging field. Proper positioning was confirmed with a 10–12-million count emission image acquired 1 min after the intravenous injection of 30 mCi of Rb-82. Nine sequential, overlapping, 1.5 cm-thick cross-sectional images of the heart and surrounding lungs were generated and used to adjust the animal's position in the camera, if necessary, so that the entire heart was placed in the center of the field of view. The position of the animal's chest was then marked with a felt pen and maintained with orthogonal low-intensity laser beams mounted on the PET camera. Following decay of ^{82}Rb, a transmission image of 200 million counts was acquired over 20 min using a ring source of ^{68}Ga around the animal for subsequent attenuation correction.

A 50-mg bolus of lidocaine was then given intravenously, followed by continuous infusion at 2 mg/min before the snare around the LAD was tightened and secured with a clamp. If ventricular fibrillation occurred, the heart was defibrillated using 50 joules via the internal paddles of a DC Physiocontrol (model #640) Defibrillator. Hypotension was treated with intravenous normal saline and dopamine infusion as needed, to maintain systolic intraarterial pressure ≥90 mmHg.

Five minutes after LAD occlusion, following hemodynamic stabilization and dose calibration, 10 mCi of ^{13}N-ammonia were given as an intravenous bolus through the right femoral vein. Image acquisition began 3 min later to allow clearance of ^{13}N activity from the blood pool. During emission imaging with ^{13}N-ammonia, a total of 40 million counts were obtained over 10–15 min. Ten to 15 min after LAD occlusion was begun, during acquisition of the perfusion image, five million well-dispersed microspheres, 15 microns in diameter labeled with ^{46}Sc (3M, Inc.) were injected over 30 sec through the left atrial catheter, while femoral arterial blood was withdrawn at approximately 7 ml/min for 3 min into a tared glass syringe using a Harvard pump.

LAD occlusion continued for 2 hr, followed by a 2-hr period of reperfusion to facilitate identification of distinct infarct borders by histochemical staining. The site of the myocardial infarction was subsequently used to confirm the location of the ischemic zone at risk. Following reperfusion, animals were sacrificed with a concentrated solution of potassium chloride, while still fully anesthetized.

Construction of LV Perfusion Maps from Microsphere Data

The heart was immediately removed, rinsed of excess blood with iced saline and trimmed of epicardial fat. The LV was dissected free of the remainder of the heart and weighed before being cut into 1-cm thick slices in planes paralleling those of the tomographic PET images. Each LV slice was incubated in a prewarmed (37–40°C), fresh, 1% solution of triphenyl tetrazolium chloride (TTC) for 45 min, and fixed in 10% formalin-saline solution to enhance color contrast before weighing and subsequent photography of the cut surface. Viable myocardium was identified by its bright red staining, while irreversibly injured tissue remained unstained (*13*).

All LV slices were completely divided into endocardial, midwall, and epicardial samples of approximately 0.5 g each for subsequent well counting of microsphere gamma activity. Each sample of the 200–300 samples per heart was weighed and assigned an identification number documenting its position within the LV wall. Gamma radioactivity was then measured in a three inch sodium iodide crystal well counter (LKB Compu Gamma) using an energy window centered over the photopeaks of ^{46}Sc. Perfusion in each myocardial tissue sample was then calculated as we have previously reported (*14*) using the method of Domenech et al. (*15*).

The perfusion map of absolute flow values derived from microsphere analysis of ^{46}Sc injected during coronary occlusion was inspected and a frequency histogram of this data constructed. Peak nonischemic flow in each animal was identified as the mean of the top 10% of perfusion values in the mid-wall of the three midventricular slices. In all animals, the tissue samples with peak perfusion were located remote from the ischemic zone. All myocardial samples with perfusion values of less than 50% of this average peak flow value were then located on the perfusion maps and their position in or near the infarct area confirmed. If the sample contained epicardial fat or valvular tissue or was anatomically distant from the infarct area and had low radioactivity, these samples were not counted as critically "ischemic" but as "wild" points and discarded. The critically ischemic LV myocardial mass was then computed as the aggregate weight of all tissue samples with perfusion less than 50% of the peak mid wall value and was expressed as a fraction of the total LV weight.

Perfusion Image Analysis

PET perfusion images obtained with ^{13}N-ammonia injected during coronary occlusion were thresholded so that only pixels with 50% or more of peak myocardial ^{13}N-ammonia uptake were displayed. Fifty percent thresholding provided a standardized, objective, and reproducible way to define LV edges in PET perfusion images and to allow extrapolation around the image defect with minimal operator judgment. Computer-assisted, hand-drawn regions of interest (ROIs) were constructed to include all pixels with myocardial ^{13}N-ammonia activity in the thresholded image. The ROIs were extrapolated to include the perfusion defect produced during coronary occlusion. The number of pixels with less than 50% of the peak ^{13}N-ammonia uptake in the myocardial images was then expressed as a fraction of the total number of pixels in the LV PET image.

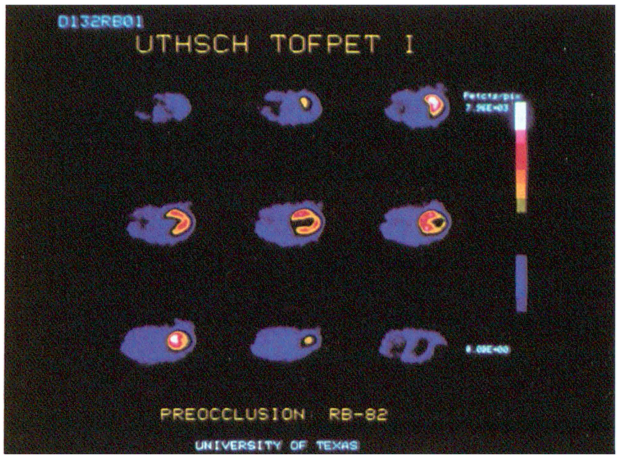

FIGURE 1. Myocardial perfusion images obtained with ^{82}Rb prior to LAD occlusion. The animal is lying on her right side with her head pointing toward the viewer. Seven of the nine slices contain activity from the LV. The base of the heart is to the left and apex to the right with cranial transaxial slices on the top row, mid-ventricular slices in the central row, and caudal slices in the lowest row.

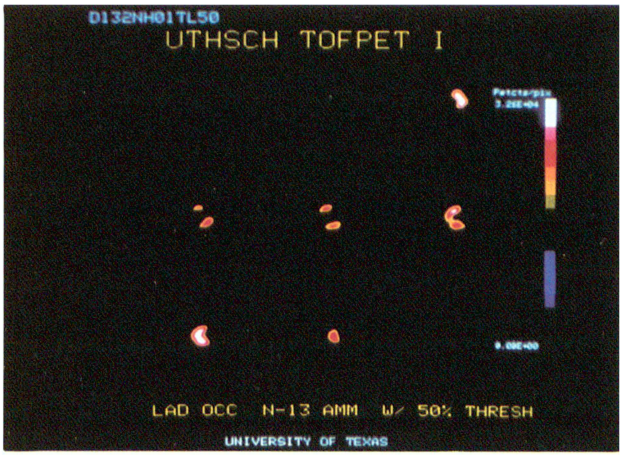

FIGURE 3. Myocardial perfusion images of Figure 2 following 50% thresholding. All background activity has disappeared and discrete LV edges including the transmural edge of the anterior-apical defect are apparent.

Statistics

Regression analysis using the least squares technique was performed with a statistical software package for the IBM PC (Minitab; Minitab, Inc.).

RESULTS

A representative nine-slice myocardial perfusion image obtained with ^{82}Rb prior to occlusion is shown in Figure 1. The corresponding ^{13}N-ammonia perfusion image obtained immediately after LAD occlusion in the same animal is reproduced in Figure 2, with the same image following 50% thresholding shown in Figure 3. With 50% image thresholding, background activity is eliminated and the LV image edge becomes apparent. These edges define the image defect within the myocardium and are used to extrapolate the endocardial and epicardial borders of the defect. Figure 4 demonstrates the extrapolation of myocardial borders in the 50% thresholded image of a single mid-ventricular slice around an apical image defect. The number of pixels within the image defect shown in pink, divided by the total number of pixels in the image represents the critically ischemic LV fractional volume in this slice as assessed by PET. Critically ischemic LV fractional

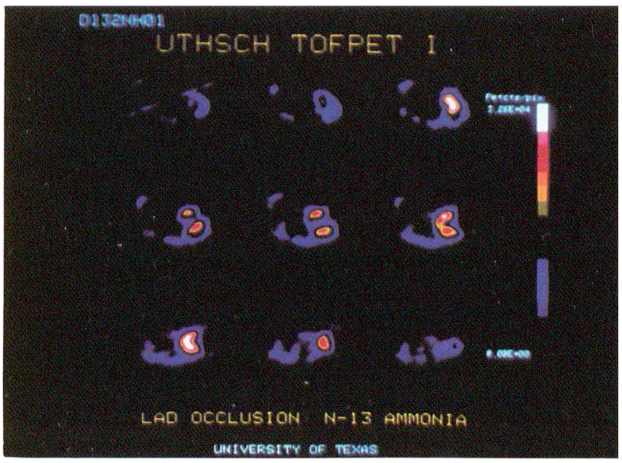

FIGURE 2. Myocardial perfusion images obtained in the same animal as in Figure 1 using ^{13}N-ammonia immediately following LAD occlusion. The animal was not moved after the pre-occlusion scan. A large apical defect is apparent, particularly in the midventricular slices. Orientation of the images is the same as in Figure 1.

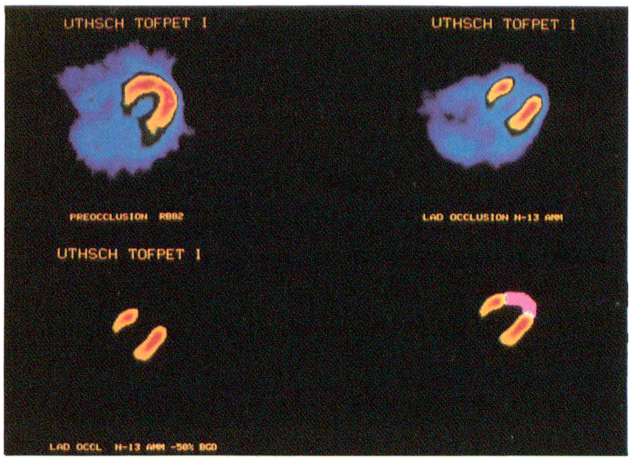

FIGURE 4. A single mid-ventricular slice of a perfusion image prior to occlusion with ^{82}Rb is on the upper left, with the ^{13}N-ammonia image immediately after occlusion on the upper right. The 50% threshold image for defining defect size is on the lower left with the defect outlined in pink on the lower right image. The number of pixels in the defect (pink) divided by the total number of LV pixels in the thresholded image, summed for all slices provides the fraction of critically ischemic LV myocardium during coronary occlusion.

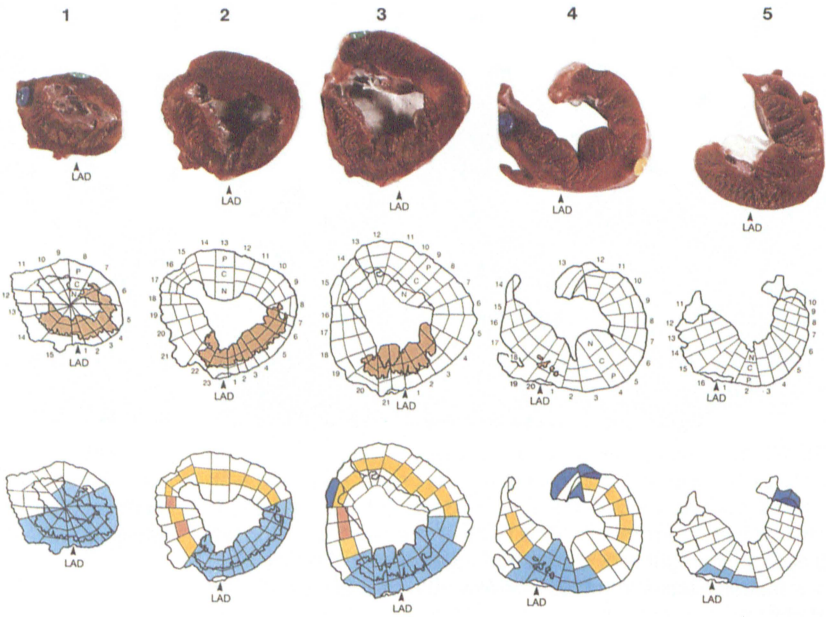

FIGURE 5. The upper row shows TTC-stained LV slices demonstrating an anteroapical subendocardial infarct (brown unstained area). The most apical slice is on the left, viewed from below at the basal surface. In the second row, the infarct zone has been outlined and a schematic map identifying the location of each LV sample for microsphere analysis drawn. Each transmural slice is numbered radially and is further subdivided into an endocardial (N), mid-wall (C), or epicardial (P) sample. In the third row, mid-wall samples in the three mid-ventricular slices are identified in yellow. Those samples showing peak perfusion (the upper 10% of the non-ischemic perfusion values) are shown in orange. All samples with less than 50% of peak perfusion are shown in blue. Dark blue samples (less than 3% of the total LV weight) indicate samples with low flow values because of inclusion of valvular apparatus or epicardial fat. These samples were omitted from the calculation of critically ischemic LV fractional mass.

volume was determined from the summed data of all image slices in each animal.

Figure 5 depicts the basal surfaces of the LV slices following LAD occlusion for 2 hr, reperfusion for 2 hr, and TTC staining for 45 min from the same animal whose perfusion images are shown in Figures 1–3. The slices are arranged consecutively from apex to base, starting with the apex on the left. A sixth slice, representing a small piece of the extreme base of the heart, is not shown. The infarcted tissue is identified in the subendocardium by its brown, unstained appearance, while viable, reversibly ischemic tissue stains bright red in the adjacent mid-wall and epicardium. Figure 5 also demonstrates the location of each ventricular myocardial sample for microsphere perfusion measurements in the same animal in relation to the site of infarction. Samples with the highest midwall flow (the upper 10% of the midwall samples of the three midventricular slices), are shown in orange and were distributed in myocardium remote from the infarct in all animals. In Figure 5, all samples with perfusion values of less than 50% of the peak, nonischemic values are shown in blue. Samples that were rejected because they were remote from the infarct or contained valvular tissue or obvious fat are identified as dark blue. Such samples comprised less than 3% of the total LV mass in all experiments.

Average peak, normal, and ischemic zone flows are shown in Table 1.

TABLE 1
Perfusion and Critically Ischemic Risk Zone Size During Coronary Occlusion

Expt no.	Perfusion (ml/min/gm ± s.d.)				Critically ischemic risk zone size (%)	
	Peak	Ischemic threshold	Critically ischemic	Nonischemic	Microspheres	PET
D77	1.19	≤0.60	0.30 ± 0.19	1.11 ± 0.12	29.1	28.8
D132	1.48	≤0.74	0.19 ± 0.21	1.22 ± 0.18	30.0	26.4
D136	1.50	≤0.75	0.37 ± 0.17	1.34 ± 0.19	13.2	16.1
D145	1.15	≤0.57	0.41 ± 0.16	1.00 ± 0.10	22.1	27.3
D178	4.20	≤2.10	1.20 ± 0.68	3.48 ± 0.53	12.2	10.5
D179	2.25	≤1.13	0.51 ± 0.34	1.81 ± 0.28	20.4	16.9
D201	1.04	≤0.52	0.27 ± 0.18	0.89 ± 0.10	22.3	20.9
D204	1.17	≤0.58	0.19 ± 0.18	1.01 ± 0.14	23.5	21.5
D229	1.00	≤0.50	0.48 ± 0.07	0.82 ± 0.10	5.0	0

Mean absolute perfusion values during coronary occlusion are presented in ml/min/g for peak, critically ischemic, and nonischemic tissue in each experimental animal. Critically ischemic risk zone size assessed by microspheres versus PET is also presented, as the percentage of total LV mass.

The weights of the critically ischemic LV samples with perfusion less than 50% of the peak value in nonischemic tissue (shown in light blue), summed and expressed as a fraction of total LV mass, ranged from 5.0% to 30.0% of the total LV weight. The proportion of total LV image volume with ^{13}N-ammonia uptake less than 50% of peak myocardial activity as determined from the 50% thresholded PET images ranged from 0% to 28.8%. The correlation between critically ischemic fractional LV mass by PET and by microspheres is shown in Figure 6. Regression analysis by least squares best fit technique demonstrated a linear correlation approximately the line of identity ($y = 1.05X - 2.0\%$) with a correlation coefficient of $r = +0.94$ with an intercept close to the origin.

DISCUSSION

This study demonstrates that the critically ischemic fraction of LV myocardium can now be measured noninvasively during acute coronary occlusion in vivo. The accuracy of this method results from the use of attenuation corrected imaging with a freely diffusible perfusion tracer to account for both antegrade and collateral flow into the ischemic zone at risk, as well as myocardial oxygen demand during coronary occlusion, reflected in the magnitude of peak flow in the nonischemic zone. Nitrogen-13-ammonia has been extensively evaluated and validated as a diffusible positron-emitting flow indicator (*1,9*) with 80% extraction during its first capillary transit due to metabolic trapping even at very low levels of flow. From approximately 0–3 ml/min/g, myocardial tissue concentration of ^{13}N-ammonia is nearly linearly related to myocardial blood flow. Thus, all three variables that determine the amount of eventual myocardial necrosis are assessed, defining the critically ischemic zone at risk physiologically, rather than purely anatomically.

The term "critical" ischemia was introduced by Hearse and Yellon based on paired flow and metabolic studies of myocardial biopsies obtained during various durations of coronary occlusion in dogs (*4*). At flows greater than 50% of normal after occlusion, ATP content after 5 min of ischemia was equivalent to that seen after a 2-hr period of flow reduction to this level. Therefore, during coronary occlusion, flow reduction by less than 50% appears to be metabolically well tolerated by ischemic tissue, presumably due to a compensatory decrease in contractile function with associated lowered metabolic demands (*16*), as well as increased oxygen extraction, and more efficient substrate utilization (e.g., anaerobic glycolysis) (*17*).

At flows lower than 50% of normal, tissue ATP content declined rapidly and linearly as flow fell further toward zero. Thus, there appears to be a flow reduction threshold beyond which metabolic and contractile compensatory factors fail to maintain an acceptable energy balance and therefore cause necrosis, a physiologic zone at risk.

Various thresholding approaches have been developed for single-photon tracers (^{99m}Tc and ^{201}Tl) and SPECT imaging systems in order to determine myocardial infarct size (*18–20*). Wolfe et al. (*18*), empirically selected pixels with less than 50% of maximal activity to define infarcted myocardium using ^{99m}Tc-pyrophosphate images. Holman and coworkers attempted to recover hypoperfused myocardial mass from ^{201}Tl images obtained with SPECT during acute coronary occlusion in dogs (*20*), but concluded that the accuracy of the technique was critically dependent upon an arbitrary and variable threshold used to define the myocardial border in perfusion images.

Weiss et al. utilized ^{11}C-palmitate and a single-slice PET camera to measure the fraction of LV myocardium infarcted 48 hr after LAD coronary occlusion (*21*). Morphologic estimates of infarct size as a percentage of the single slice correlated closely with estimates from single PET tomographs in six animals ($r = 0.97$) after 50% thresholding of the images. These authors found good ($r = 0.92$) correlation between CK-MB estimates and PET estimates of infarct size in 13 patients with transmural anterior or lateral infarction (*22*) when the 50% threshold was used to define endocardial and epicardial borders of normal myocardium and the edges of infarcted tissue using a multi-slice PET camera and ^{11}C-palmitate.

In the present study of the critically ischemic zone at risk, a fixed threshold of 50% was chosen to define all myocardial borders, i.e., epicardial and endocardial edges of the heart as well as the lateral borders of the ischemic zone. Since recovery of hypoperfused LV mass was determined as a percentage of total LV mass in the same image, errors in absolute quantification due to inaccurate detection of myocardial edges resulting from cardiorespiratory motion, spillover of activity from blood pool and background, and partial volume effects were minimized, being present in both the normally perfused and ischemic areas.

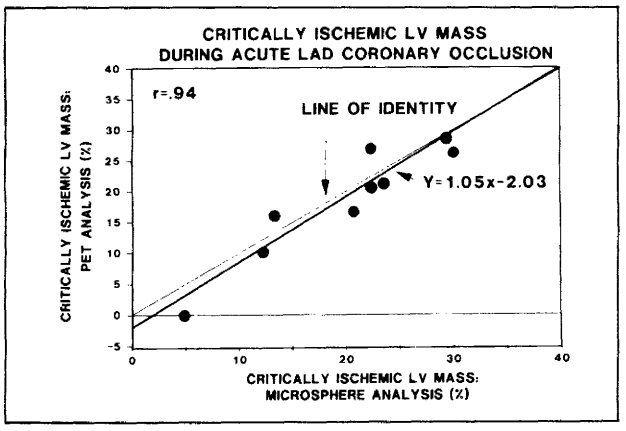

FIGURE 6. Correlation between critically ischemic fractional LV mass determined in vitro by microsphere analysis versus in vivo from thresholded PET perfusion images. The regression line approximates the line of identity.

Limitations of This Study

The minimal operator interaction undoubtedly involves error in the measurement of ischemic fractional mass

directly from PET images. Perfusion imaging with PET failed to detect a critically ischemic fractional LV mass of 5% or less, probably due to spillover of activity from adjacent myocardium into the image defect due to partial volume effects and the relatively poor resolution of the imaging system used. Detection of very small, critically ischemic image defects may be improved in the larger human heart because of less severe partial volume constraints, and with the higher resolution PET imaging systems (e.g., 6–8 mm FWHM) now available.

This experimental model used LAD occlusion producing apical defects. With basal or inferior defects, extrapolation may be more difficult if the original transaxial tomographs are used for analysis. Potential solutions include the addition of blood pool imaging (e.g., with ^{15}O or ^{11}C-carbon monoxide) to define the endocardial border of perfusion defects and three dimensional image reconstruction of true short-axis and long-axis views. Automatic thresholding and edge detection by artificial intelligence techniques should further improve both speed and accuracy of this approach for routine clinical application (*23,24*).

CONCLUSIONS

In this study, we describe a method using a diffusible perfusion tracer and attenuation corrected PET imaging to define the fraction of LV myocardium that has flow reduction severe enough, 50% of normal or less, to place the tissue at risk for cellular injury, thus defining the physiologic zone at risk noninvasively. The critically ischemic LV mass determined with this method directly from PET images in vivo correlated well with microsphere determinations in vitro.

The ability to accurately recover critically ischemic myocardial fractional mass in vivo using this method may be of significant value in objectively assessing the efficacy of myocardial salvage strategies in man. Further studies in the clinical environment are necessary to define its utility in that setting.

ACKNOWLEDGMENTS

The authors would like to acknowledge the technical assistance of Mr. Jonathan McLean as well as the secretarial assistance of Ms. Claire Finn, Ms. Kathryn Rainbird, and Mrs. Karen Swann, who were kind enough to type the manuscript.

This work was supported in part by NIH grants ROI HL26862, HL26885, AHA grant TXR253 and as a joint collaborative project with the Clayton Foundation for Research.

REFERENCES

1. Schelbert HR, Phelps ME, Huang SC, et al. N-13-ammonia as an indicator of myocardial blood flow. *Circulation* 1981;63:1259–1272.
2. Goldstein RA, Mullani NA, Marani SK, Fisher DJ, Gould KL, O'Brien HA. Myocardial perfusion with rubidium-82. II. Effects of metabolic and pharmacologic interventions. *J Nuc Med* 1983;24:907–915.
3. Goldstein RA, Mullani NA, Wong WH, et al. Positron imaging of myocardial infarction with rubidium-82. *J Nucl Med* 1986;27:1824–1829.
4. Hearse DJ, Crome R, Yellon DM, Wyse R. Metabolic and flow correlates of myocardial ischemia. *Cardiovasc Res* 1983;17:452–458.
5. Goldstein RA, Kirkeeide R, Demer L, et al. Relations between geometric dimensions of coronary artery stenoses and myocardial perfusion reserve in man. *J Clin Invest* 1987;79:1473–1478.
6. Demer LL, Gould KL, Goldstein RA, et al. Assessment of coronary artery disease severity by positron emission tomography: Comparison to quantitative arteriography in 193 patients. *Circulation* 1989;79:825–835.
7. Gould KL. Identifying and measuring severity of coronary artery stenosis. Quantitative coronary arteriography and positron emission tomography. *Circulation* 1988;68:237–245.
8. Demer LL, Goldstein R, Mullani N, et al. Coronary steal by noninvasive PET identifies collateralized myocardium [Abstract]. *J Nucl Med* 1986;27:977.
9. Schelbert HR, Phelps ME, Hoffman EF, Huang S, Selin CE, Kuhl DE. Regional myocardial perfusion assessed with N-13-labeled ammonia and positron emission computerized axial tomography. *Am J Cardiol* 1979;43:209–218.
10. Vaalburg W, Kamphuis JA, Berling-Van Der Molen HB, Reiffon S, Rijskamp A, Woldring MG. An improved method for the cyclotron production of ^{13}N-labeled ammonia. *Int J Appl Rad Isot* 1975;26:316–318.
11. Neirinckx RD, Kronauge JF, Gennaro GP. Evaluation of inorganic absorbents for rubidium-82 generator: I. Hydrous SnO_2. *J Nucl Med* 1982;24:898–906.
12. Mullani NA, Gaeta J, Yerian K. Dynamic imaging with high resolution time-of-flight PET camera—TOFPET I. *IEEE Trans Nucl Sci* 1984;31:609–613.
13. Fishbein MC, Meerbaum S, Rit J, et al. Early phase acute myocardial infarct size quantification: validation of the triphenyl tetrazolium chloride tissue enzyme staining technique. *Am Heart J* 1981;101:593–600.
14. Merhige ME, Smalling RW, Cassidy D, et al. Effect of the hemopump left ventricular assist device on regional myocardial perfusion and function: Reduction of ischemia during coronary occlusion. *Circulation* 1989;80 (suppl III):158–166.
15. Domenech RJ, Hoffman JI, Noble MI, Saunders KB, Hensen JR, Subijanto S. Total and regional coronary blood flow measured by radioactive microspheres in conscious and anesthetized dogs. *Circulation Res* 1969;25:581–596.
16. Vatner SF. Correlation between acute reductions in myocardial blood flow and function in conscious dogs. *Circulation Res* 1983;17:452–458.
17. Guth BD, Martin JF, Heusch G, Ross J Jr. Regional myocardial blood flow, function and metabolism using phosphorus-31 nuclear magnetic resonance spectroscopy during ischemia and reperfusion in dogs. *J Am Coll Cardiol* 1987;10:673–681.
18. Wolfe CL, Lewis SE, Corbett JR, Parkey RW, Buja M, Willerson JT. Measurement of myocardial infarction fraction using single-photon emission computed tomography. *J Am Coll Card* 1985;6:145–151.
19. Tamaki S, Nakajima H, Murakami T, et al. Estimation of infarct size by myocardial emission computed tomography with thallium-201 and its relation to creatine kinase-MB release after myocardial infarction in man. *Circulation* 1982;66:994–1001.
20. Holman BL, Moore SC, Shulkin PM, Kirsch C, English RJ, Hiu TC. Quantitation of perfused myocardial mass using T1-201 and emission computed tomography. *Invest Radiology* 1983;18:322–326.
21. Weiss ES, Ahmed SA, Welch MJ, Williamson JR, Ter-Pogossian MM, Sobel BE. Quantification of infarction in cross sections of canine myocardium *in vivo* with positron emission transaxial tomography and ^{11}C-palmitate. *Circulation* 1977;55:66–73.
22. Ter-Pogossian MM, Klein MS, Markham J, Roberts R, Sobel BE. Regional assessment of myocardial metabolic integrity in vivo by positron emission tomography with ^{11}C-labeled palmitate. *Circulation* 1980;61:242–255.
23. Rowe RW, Merhige ME, Bendriem B, Gould KL. Region of interest determination for quantitative evaluation of myocardial ischemia from PET images. In: de Graaf CN and Viergeven MA, ed. *Information processing in medical imaging*. New York: Plenum Publishing Corp., 1988:591–600.
24. Hicks K, Rowe RW, Gould KL. Techniques to enhance interpretation of functional cardiac images from PET. From the proceedings of the 9th annual conference of the IEEE Engineering in Medicine and Biology Society, Boston, MA, 1987;2:846.